J. Coat. Technol. Res., **17** (5) 1401–1411, 2020
https://doi.org/10.1007/s11998-020-00360-1

A facile strategy to fabricate an intumescent fire-retardant coating with improved fire resistance and water tolerance for steel structure

Siqi Huo, Cheng Wang, Qinghua Hu, Shi Liu, Qi Zhang, Zhitian Liu

Abstract An intumescent fire-retardant coating (IFRC) with improved fire resistance and water tolerance was prepared in this work, resulting from the introduction of microcapsuled ammonium polyphosphate (MFAPP) and zinc borate (MFBZ). The as-prepared coating exhibited great fire resistance and smoke suppression. In the cone calorimetry test, adding only 6 wt% MFBZ dramatically reduced the peak heat release rate, total heat release, and total smoke release by $\sim$ 23.4%, $\sim$ 54.7%, and $\sim$ 81.1%, respectively. In addition, the water resistance and thermal stability of the coatings were also characterized. The char yield of IFRC noticeably increased to 41.7%, indicating good high-temperature stability. Besides, the IFRC showed a water contact angle of 90.1° and maintained good structure and fire resistance after being soaked by water, indicating great water resistance. The enhanced performance portfolio was mainly due to the synergistic effects of ammonium polyphosphate, pentaerythritol, melamine, and zinc borate, and the hydrophobicity of melamine–formaldehyde resin (MF). This work offers an effective approach for the preparation of waterborne intumescent fire-retardant coatings with great fire resistance and water tolerance.

Electronic supplementary material The online version of this article (https://doi.org/10.1007/s11998-020-00360-1) contains supplementary material, which is available to authorized users.

S. Huo, C. Wang, Q. Hu, S. Liu, Q. Zhang (✉), Z. Liu (✉)
Institute of Materials for Optoelectronics and New Energy, School of Materials Science and Engineering, Wuhan Institute of Technology, Wuhan 430205, Hubei, People's Republic of China
e-mail: whzq_2014@163.com

Z. Liu
e-mail: able.ztliu@wit.edu.cn

Graphic abstract

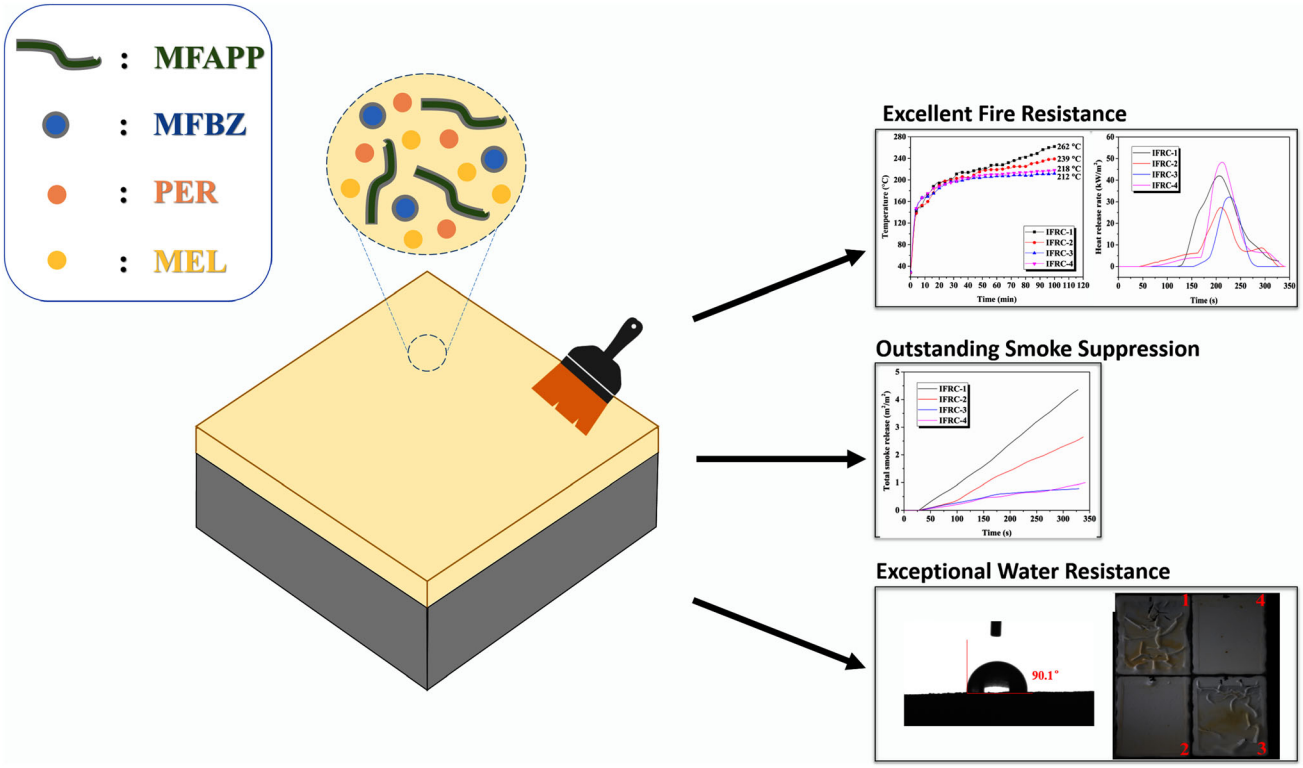

Keywords Microencapsulation, Intumescent fire-retardant coatings, Fire resistance, Thermal stability, Water tolerance

Introduction

The steel structure is an important part of a building due to its high strength-to-weight ratio, simple and convenient manufacture, and good plastic toughness.[1–4] Although steel is one kind of non-combustible material, its strength and elastic coefficient will dramatically decrease in the fire, and its strength and hardness will be completely lost when the temperature increases to 600°C.[5–6] Therefore, it is necessary to take measures to protect the steel structure from collapsing in a fire.[7] Nowadays, intumescent fire-retardant coatings are regarded as one of the most practical methods to provide passive fire protection to the structural steel.[8]

Intumescent fire-retardant coatings mainly consist of polymer binders, intumescent flame retardant (IFR), and other additives.[9–11] The traditional IFR is comprised of three parts, namely carbon source (e.g. pentaerythritol),[12,13] acid source (e.g., ammonium polyphosphate),[14] and blowing agent (e.g. melamine).[15,16] During combustion, IFR dehydrates and carbonizes to form an intumescent char layer with a shielding effect, which isolates the transmission of air and heat to protect the steel structure.[17] Unfortunately, the intumescent char layer derived from IFR is easily destroyed in a fire, leading to poor fire resistance, which seriously restricts its industrial applications.[18] Therefore, it is necessary to explore synergistic flame retardants to cooperate with IFR to endow coatings with excellent fire resistance.[19]

As an inorganic filler, zinc borate (BZ) is regarded as an effective synergistic flame retardant with smoke suppressing effect for IFR.[20–22] Under high temperature, zinc borate will degrade to generate lots of water and thermally stable boron-containing compounds. These thermally stable compounds will collaborate effectively with IFR in the formation of a compact and intumescent char layer, which isolates heat transfer and smoke diffusion during combustion.[23,24] Therefore, the introduction of zinc borate is considered as an effective way to improve the fire resistance of intumescent fire-retardant coatings.[25] However, in practical application, the coatings are often under attack by water and moisture.[26] Unfortunately, both ammonium polyphosphate and zinc borate suffer from poor water resistance.[27,28] In our previous work, we successfully used the microencapsulation technology to suppress the hydrophilia of ammonium polyphosphate and prepared an intumescent fire-retardant coating with improved water resistance, but the fire resistance of the obtained coatings was not good enough.[7] Inspired by the synergy of zinc borate and IFR, we added zinc borate into the

intumescent fire-retardant coatings to improve the fire resistance in this work. Additionally, considering the poor water resistance of zinc borate, we also modified zinc borate via microencapsulation technology.

Therefore, we fabricated an intumescent fire-retardant coating with great fire resistance and water tolerance via the introduction of microcapsuled ammonium polyphosphate and microcapsuled zinc borate in this work. The fire resistance, smoke suppression, thermal stability, and water tolerance of the coatings were comprehensively investigated. Our results showed that the as-prepared coatings featured great fire resistance, smoke suppression, and water tolerance. Thus, this work provides an easy-to-realize method for creating intumescent fire-retardant coatings with improved fire resistance, smoke suppression, and water tolerance, which has broad application prospects.

Experimental

Materials

BZ ($2\ ZnO{\cdot}3\ B_2O_3{\cdot}3.5\ H_2O$) was purchased from Shandong Xiucheng Chemical Co., Ltd. Formaldehyde (37 wt% solution) was provided by Nanjing Chemical Reagent Co., Ltd. Poly(methyl methacrylate-butyl acrylate)/poly(methyl methacrylate-butyl acrylate-methacrylic acid) as soft-core/hard-shell emulsion was prepared in our lab.[7] Polyethylene glycol octylphenol ether, ammonium polyphosphate (APP, $n > 1000$), pentaerythritol (PER), melamine (MEL), and sodium bicarbonate ($NaHCO_3$) were obtained from Sinopharm Chemical Reagent Co., Ltd. Hydrochloric acid (HCl) was purchased from Xinyang Chemical Reagent Factory. All the reagents were used as received.

Sample preparation

Preparation of MFAPP

The microencapsulated APP with melamine formaldehyde resin (MFAPP) was prepared according to our previous research.[7]

Preparation of MFBZ

(a) Preparation of suspension

The mixture of 100 mL of ethanol and 0.5 g of polyethylene glycol octylphenol ether were added into a round-bottom glass flask with a magnetic stirrer. Then, 21 g of BZ was slowly added into the flask with continuous stirring for 1 h to obtain BZ suspension.

(b) Preparation of melamine–formaldehyde resin

In a 250 mL round-bottom flask, 6.3 g of melamine was dispersed in 12.1 g of formaldehyde solution through stirring at room temperature and the molar ratio of melamine/formaldehyde was 1:3. Then, $NaHCO_3$ with a mass concentration of 10% was dropped into the solution to adjust the pH value to about 8–9. The mixed solution was heated to 70°C and then stirred for 0.5 h to obtain melamine formaldehyde resin.

(c) Preparation of microencapsulated zinc borate

In a three-necked round-bottom flask, the as-prepared BZ suspension was dispersed in the melamine–formaldehyde resin by vigorously stirring. Dilute hydrochloric acid solution was added into the flask to adjust the pH value to approximately 4–5. Then, the mixture was heated to 70–80°C and kept for 2 h. After being cooled to room temperature, the crude product was obtained by filtration. Finally, the crude product was washed with distilled water and dried at 60°C to obtain the microencapsulated zinc borate with melamine formaldehyde resin (MFBZ).

Preparation of intumescent fire-retardant coatings

The formulations of intumescent fire-retardant coatings are listed in Table 1. All raw materials for coatings were grinded for 1 h in an agate mortar. For the fire resistance test, the as-prepared coatings were brushed on one side of a steel plate with the size of $150 \times 100 \times 3\ mm^3$ and dried at room temperature

Table 1: The compositions of intumescent fire-retardant coatings

Compositions	IFRC-1	IFRC-2	IFRC-3	IFRC-4	IFRC-5	IFRC-6	IFRC-7
Emulsion (%)	18.6	18.6	18.6	18.6	18.6	18.6	18.6
PER (%)	15.2	15.2	15.2	15.2	15.2	15.2	15.2
MEL (%)	10.8	10.8	10.8	10.8	10.8	10.8	10.8
Promoters (%)	2.2	2.2	2.2	2.2	2.2	2.2	2.2
Water (%)	25.0	23.0	19.0	15.0	19.0	19.0	19.0
APP (%)	–	–	–	–	28.2	–	28.2
MFAPP (%)	28.2	28.2	28.2	28.2	–	28.2	–
BZ (%)	–	–	–	–	6.0	6.0	–
MFBZ (%)	0	2.0	6.0	10.0	–	–	6.0

for 72 h. This process was repeated for several times until the film thickness reached 1 ± 0.1 mm. For the cone calorimeter test, the as-prepared coatings were brushed on one side of a steel plate with the size of 100 × 100 × 3 mm^3 and dried at room temperature for 72 h.[29] This process was repeated for several times until the film thickness reached 2 ± 0.1 mm.

Characterization

Fourier transform infrared spectroscopy (FTIR)

The Fourier transform infrared spectra (FTIR) were recorded on Nicolet 6700 FT-IR spectrophotometer (Perkin Elmer Company, USA) in the range of 400–4000 cm^{-1} using KBr pellet.

Particle size distribution

The mean particle size and distribution of BZ and MFBZ were measured by Malvern Zetasizer Nano Series Nano-ZS. Before testing, the samples were dispersed in ethanol and sonicated for 15 min.

Scanning electron microscopy (SEM)

Scanning electron microscopy (SEM) images were obtained by using AMARY 1000 SEM with an acceleration voltage of 20 kV.

Solubility in water of BZ and MFBZ

Water solubility was determined by adding 5 g samples into 100 mL distilled water and stirring separately at 25, 50, and 75°C for 24 h. After centrifugal filtration of suspension, 20 mL filtrate was taken out and dried to a constant weight (m) at 90°C. Water solubility of sample was calculated according to the following equation:

$$R = m/20 \times 100$$

Contact angle analysis

The contact angles of water drop on samples were measured by a contact angle goniometer (DSA100, KRUSS Company, Germany) at room temperature.

The static immersion test

The static immersion test was used as an accelerated aging test of water on the coating. Before the test, the coatings were brushed on the surface of tinplate. After sealing the borders with paraffin, the whole plate was dried at room temperature for 72 h. The dried board was immersed in distilled water at room temperature for 72 h and recorded with a digital camera. The obtained plates were dried at room temperature for 72 h and then used for the fire resistance test.

Fire resistance test

The torch fire test was used to evaluate the heat shielding performance of the coatings in our laboratory according to the ASTM E119 standards. The setup for investigating the fire shielding performance of fire-retardant coatings is shown in Fig. S1. The coatings on the steel substrate were burned by a brass coal gas burner, which offered a high-temperature flame (about 1000°C). The distance between the coating and burner was maintained at 7 cm, and the pressure of burner outlet was kept at 0.09–0.10 MPa. The backside temperature of substrate was recorded through the thermocouple once a minute for 100 min. For each coating, the test was repeated 2–3 times to ensure the accuracy of the data.

Cone calorimeter test

A cone calorimeter (Stanton Redcroft, UK) was used to investigate the combustion behaviors of samples with the dimension of 100 mm × 100 mm × 3 mm. The samples were detected according to ISO 5660 standard and exposed to an external heat flux of 50 kW/m^2.

Thermogravimetric analysis (TGA)

Thermogravimetric analysis (TGA) was studied by using NETZSCH STA409PC LUXX under a N_2 flow. Samples (about 5 mg) were heated from 40 to 800°C at a heating rate of 10°C/min.

Results and discussion

Characterization of MFBZ

The FTIR spectra of BZ, MF resin, and MFBZ are presented in Fig. 1a. Typical absorption peaks of BZ were observed at 1400, 1300, 1186, 1079, 960, and 750 cm^{-1}, corresponding to the asymmetric stretching vibrations of trihedral borate (BO_3) and tetrahedral borate (BO_4) groups and the symmetric stretching vibrations of BO_3 and BO_4 groups.[30,31] With regard to MFBZ, main absorption peaks appeared at 1484, 1400, 1300, 1186, 1079, 960, 815, and 750 cm^{-1}, respectively. The absorption peaks located at 1484 and 815 cm^{-1}

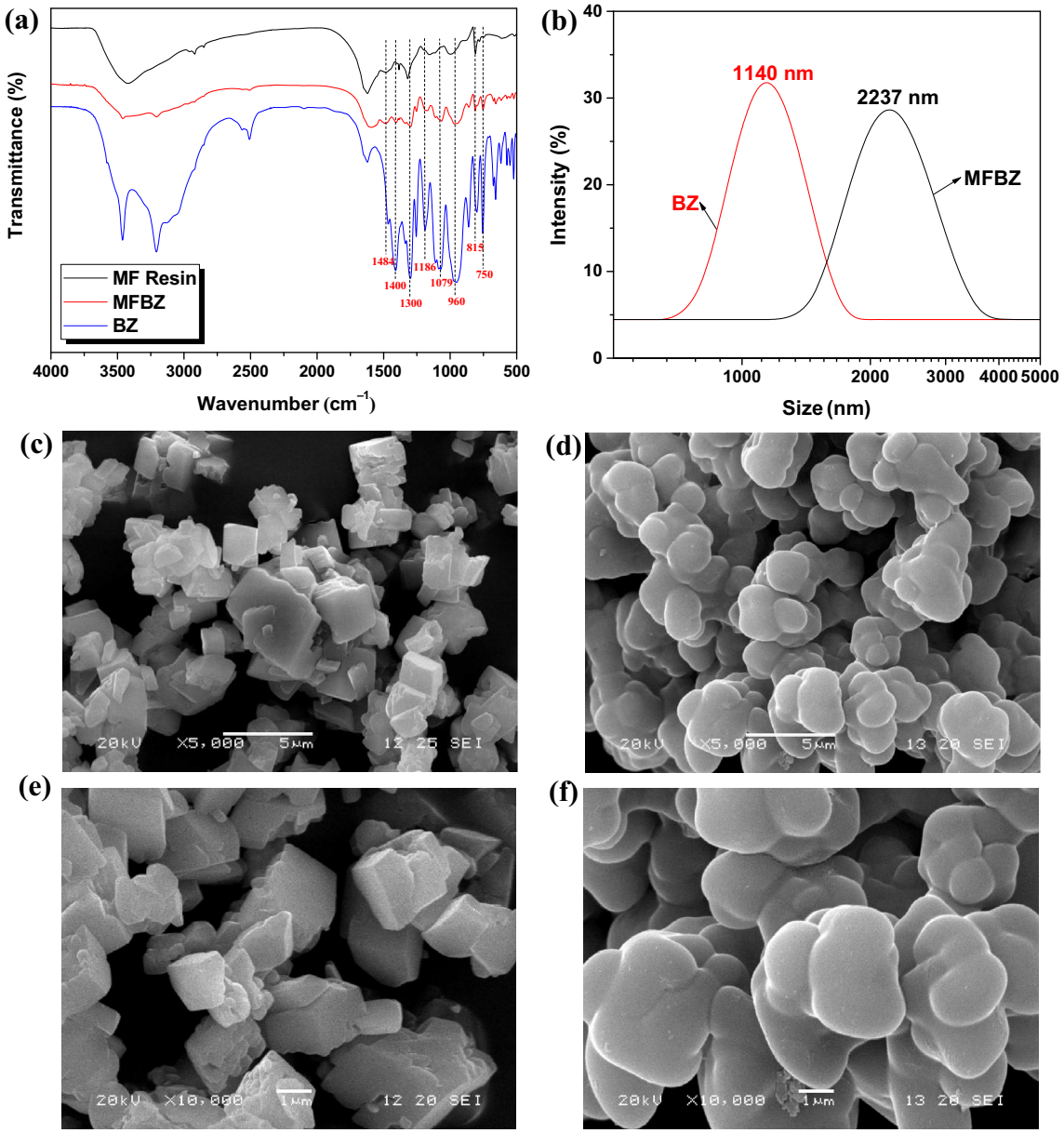

Fig. 1: (a) FTIR spectra of MF resin, MFBZ, and BZ, (b) particle size distributions of BZ and MFBZ, and SEM images of (c, e) BZ and (b, d) MFBZ under different resolutions

were attributed to the blending vibrations of C-H and the ring vibrations of melamine from the MF resin.[32] The FTIR spectrum of MFBZ displayed the characteristic absorption peaks of BZ as well as MF resin, indicating their existence in the MFBZ.

The particle size distributions of BZ and MFBZ are shown in Fig. 1b. The average diameter of MFBZ (2237 nm) was much larger than that of BZ (1140 nm), indicating that MF resin had been wrapped onto the surface of BZ particles. Moreover, the variations in particle size distribution also confirmed the successful preparation of MFBZ.

To study the difference in surface morphology of BZ and MFBZ, scanning electron microscopy (SEM) was performed. As shown in Figs. 1c and 1e, BZ exhibited an irregular cubic solid structure with sharp edges. However, the surface of MFBZ was smooth, and it displayed a globular solid structure without sharp edge in Figs. 1d and 1f. This obvious change further proved the successful preparation of MFBZ, which was consistent with the FTIR and particle size results.

The thermal decomposition behaviors of BZ, MFBZ, and MF resin were investigated using thermogravimetric analysis (TGA) with the corresponding curves shown in Fig. 2a. The thermal decomposition of BZ mainly occurred from 300–500°C, which was ascribed to the dehydration of the zinc borate.[33] For MF resin, there were three thermal decomposition

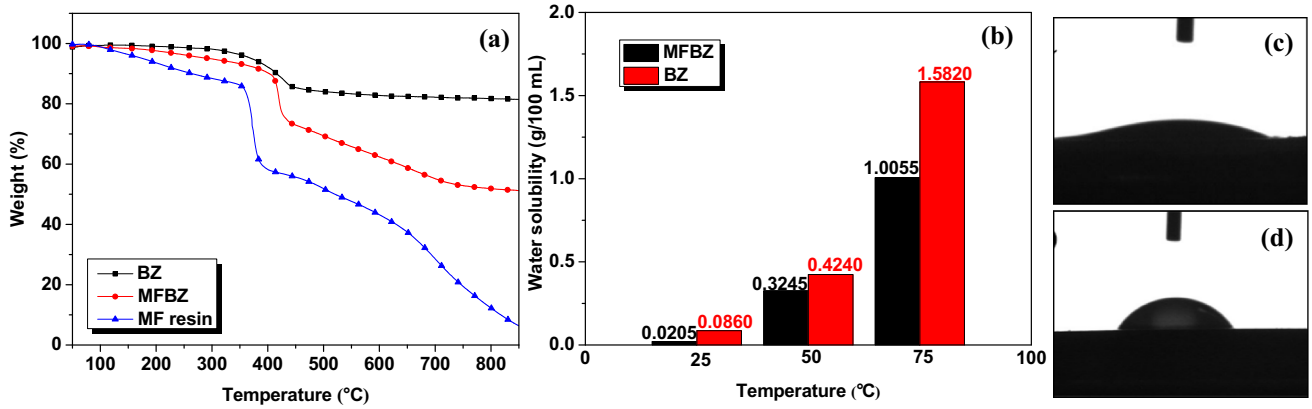

Fig. 2: (a) TGA curves of BZ, MFBZ and MF resin, (b) water solubility of MFBZ and BZ, and water contact angle of (c) BZ and (d) MFBZ

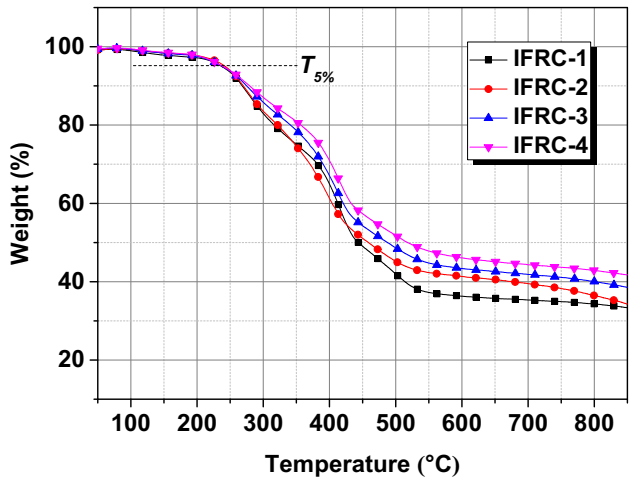

Fig. 3: TGA curves of IFRC-1, IFRC-2, IFRC-3, and IFRC-4

stages. The first degradation step (before 280°C) was due to the evaporation of water in MF resin.[34] The second degradation stage (280–450°C) was attributed to the release of NH_3 and CO_2. The last stage (450–850°C) was caused by the further decomposition of MF resin. Obviously, MFBZ exhibited similar thermal decomposition behavior to BZ below 400°C, while the thermal decomposition of MFBZ had obviously changed in 400–850°C because of the microencapsulation. It was worth noting that the char yield of MFBZ was as high as 51.2% at 850°C, which contributed to working together with IFR in the formation of a protective intumescent char layer under external flame.

The microencapsulation was aimed to improve the water resistance of BZ, and thus, it was necessary to investigate the difference of water solubility between MFBZ and BZ. Hence, the water solubility of BZ and MFBZ at 25, 50, and 75°C was investigated and the corresponding results are presented in Fig. 2b. After the microencapsulation, the water solubility of MFBZ was decreased by ~ 76.2%, ~ 23.5%, and ~ 36.4% at 25, 50, and 75°C, respectively, indicating enhanced water resistance. The significant improvement in water resistance was mainly because the hydrophobic shell MF resin could effectively protect the inner BZ particles from being attacked by water or moisture. Therefore, MFBZ with enhanced water resistance was more suitable for the application in intumescent coatings than BZ. To further study the water resistance of MFBZ, the water contact angle analysis of BZ and MFBZ was performed, with the results shown in Figs. 2c and 2d. The water contact angle for BZ was only 11.2°, while that for MFBZ increased to 46.3°, further indicating that the water resistance of BZ was improved via the microencapsulation.

Based on the results mentioned above, MFBZ with enhanced water resistance had been successfully fabricated.

Thermal properties of coatings

The influence of MFBZ on the thermal stability of coatings was studied by TGA, with the corresponding curves presented in Fig. 3. In this work, the initial decomposition temperature was defined as the temperature at 5% weight loss ($T_{5\%}$). As shown in Fig. 3, the $T_{5\%}$ for IFRC-1 without MFBZ was 236°C. With the introduction of MFBZ, the intumescent coatings exhibited similar $T_{5\%}$ (238–242°C) to IFRC-1 without MFBZ, indicating that MFBZ did not disturb the initial decomposition of coatings. Notably, MFBZ significantly improved the char yields of coatings at 850°C. For instance, the char yield of IFRC-4 increased from 33.7% to 41.7% with an enhancement of ~ 23.7%. The results indicated that the introduction of MFBZ remarkably enhanced the charring capability of coatings. The significant enhancement in charring capability contributed to improving the fire resistance.[35,36]

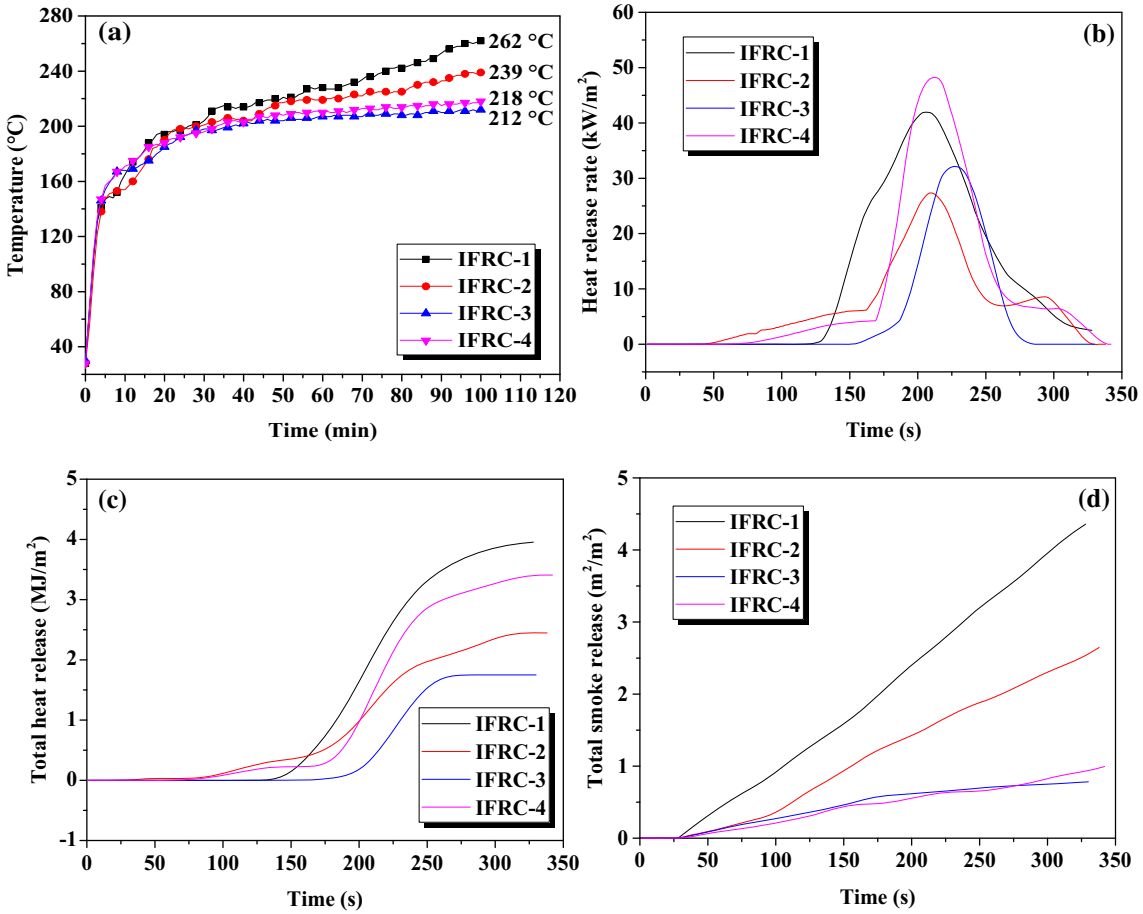

Fig. 4: Plots of (a) backside temperature, (b) heat release rate, (c) total heat release, and (d) total smoke release as a function of time

Table 2: Detailed experimental results obtained from fire resistance and cone calorimeter tests

Coating	T_{200}[a] (min)	BT_{100}[a] (°C)	T_{PHRR}[b] (s)	PHRR[b] (kW/m^2)	THR[b] (MJ/m^2)	TSR[b] (m^2/m^2)
IFRC-1	26	262	206	41.9	3.86	3.96
IFRC-2	28	239	209	27.4	2.35	2.30
IFRC-3	33	212	227	32.1	1.75	0.75
IFRC-4	39	218	212	48.2	3.27	0.83

[a] T_{200}: time to the backside temperature of 200°C, and BT_{100}: backside temperature at 100 min

[b] T_{PHRR}: time to peak heat release rate, PHRR: peak heat release rate, THR: total heat release at 300 s, and TSR: total smoke release at 300 s

Fire resistance and combustion behaviors of coatings

The fire resistance and combustion behaviors of coatings with or without MFBZ were studied by fire resistance and cone calorimeter tests. The plots of backside temperature as a function of time are shown in Fig. 4a, with the detailed results listed in Table 2. IFRC-1 without MFBZ exhibited a backside temperature of 200°C at 26 min, and its backside temperature finally reached up to 262°C at 100 min. The time (T_{200}) where the backside temperature reached 200°C was significantly delayed with the introduction of MFBZ. For instance, IFRC-3 containing only 6 wt% of MFBZ displayed a T_{200} of 39 min with a 13 min delay. In addition, the introduction of MFBZ led to a remarkable decrease in the backside temperature at 100 min. At 100 min, the backside temperature for IFRC-3 was

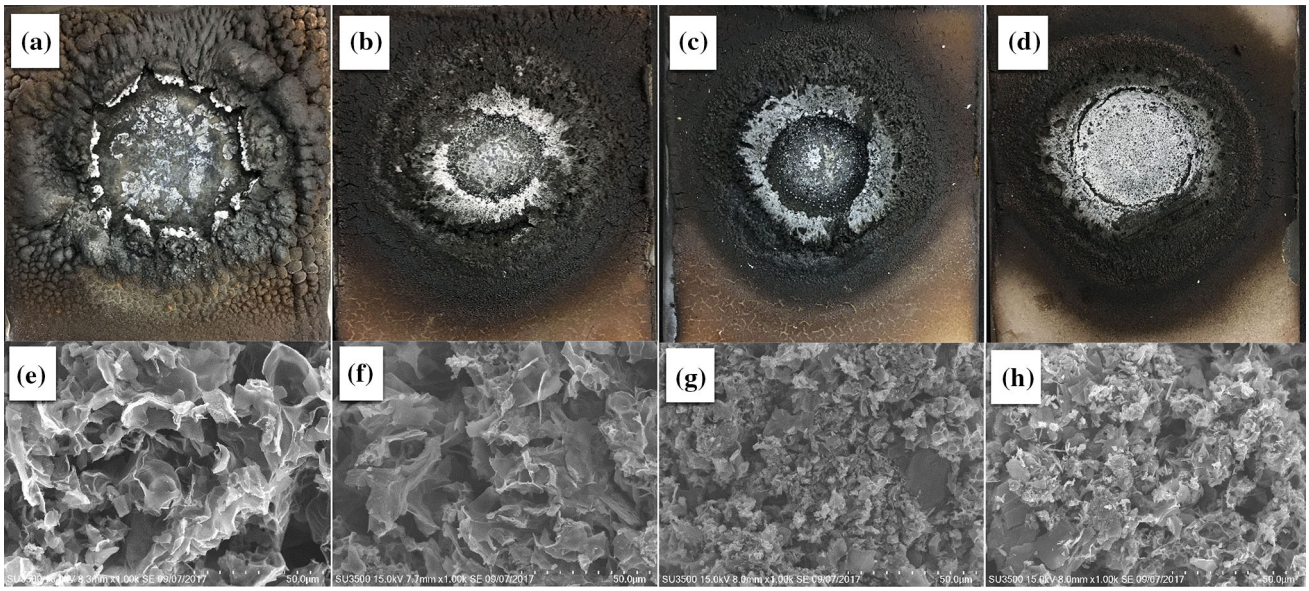

Fig. 5: Digital photographs of char residue for (a) IFRC-1, (b) IFRC-2, (c) IFRC-3, and (d) IFRC-4, and SEM images of char residue for (e) IFRC-1, (f) IFRC-2, (g) IFRC-3, and (h) IFRC-4

212°C with a reduction of 50°C, and that of IFRC-4 was 218°C with a decline of 44°C. When exposed to flame, the thermally stable products generated by the decomposition of MFBZ strengthened the compactness and thermal insulation of the char layer from IFR. Therefore, the introduction of MFBZ contributed to improving the fire resistance of intumescent coating.

The curves of heat release rate (HRR), total heat release (THR), and total smoke release (TSR) as a function of time are shown in Figs. 4b–4e. From Fig. 4b and Table 2, the heat release rate of IFRC-1 reached a peak value of 41.9 kW/m^2 at 206 s. The introduction of MFBZ remarkably delayed the T_{PHRR} and decreased the PHRR. For instance, the T_{PHRR} and PHRR of IFRC-2 were only 209 s and 27.4 kW/m^2, respectively. The PHRR values for coatings with different amounts of MFBZ decreased by 23.4–34.6% compared with the coating without MFBZ. A similar phenomenon was also observed in THR of coatings. The THR of IFRC-1 without MFBZ was as high as 3.86 MJ/m^2, while those of IFRC-2 and IFRC-3 were only 2.35 and 1.75 MJ/m^2, with reductions of $\sim$ 39.1% and $\sim$ 54.7%, respectively. The results indicated that the addition of MFBZ significantly reduced the heat release of intumescent coatings and thus improved the fire resistance.

Smoke suppression of flame retardant material is a significant parameter in fire safety fields.[37] IFRC-1 exhibited the highest TSR value of 3.96 m^2/m^2 among all coatings. It was worth noting that the addition of MFBZ brought about a remarkable reduction in the TSR of coatings. For IFRC-3, its TSR decreased from 3.96 m^2/m^2 of IFRC-1 to 0.75 m^2/m^2, with a reduction of about 81.1%, indicating the excellent smoke suppressing effect of MFBZ. This effect was also reported in other BZ-containing flame retardant systems.[38,39] However, compared with the IFRC-3, IFRC-4 exhibited slightly increased TSR, which was probably because the excessive MFBZ could not evenly disperse in the coating matrix, disturbing IFR to form the intumescent char residue during combustion and leading to inferior fire resistance and smoke suppression. In general, the incorporation of MFBZ could simultaneously confer the intumescent fire-retardant coating with great fire resistance and smoke suppression.

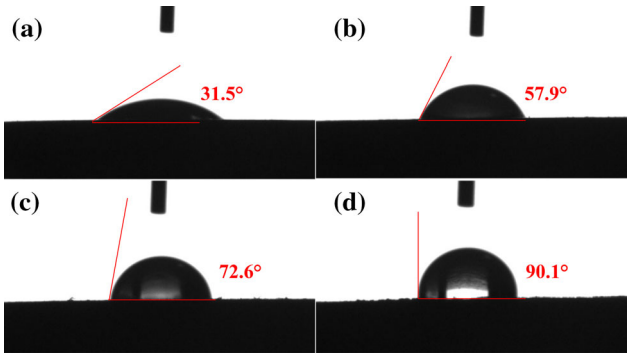

Fig. 6: The water contact angle of (a) IFRC-5, (b) IFRC-6, (c) IFRC-7, and (d) IFRC-3

Char morphology

To investigate the flame retardant mechanism, the char morphology after the fire resistance test was analyzed, and the digital photographs and SEM images of char layers are shown in Fig. 5. As shown in Fig. 5a, the char layer of IFRC-1 exhibited an intumescent structure after the fire resistance test. With the addition of MFBZ, the swelling level decreased, while the compactness increased. On the other hand, IFRC-1 exhib-

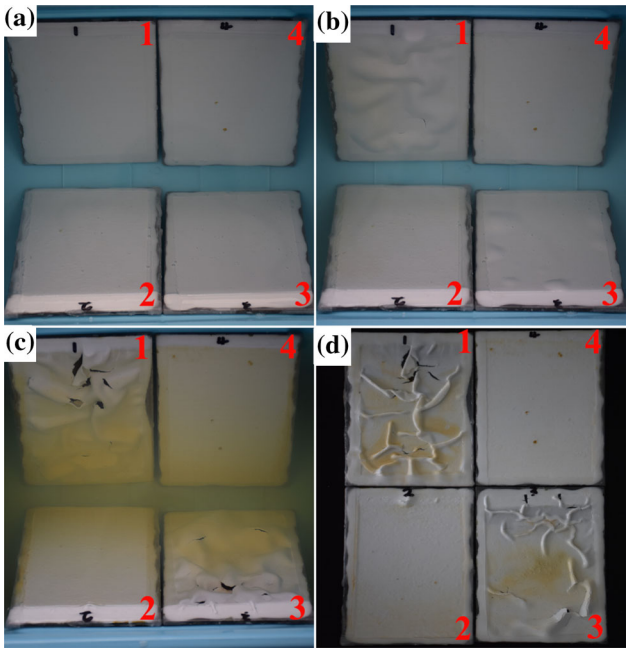

Fig. 7: The status of (1) IFRC-5, (2) IFRC-6, (3) IFRC-7, and (4) IFRC-3 after being soaked for (a) 0 h, (b) 2 h, and (c, d) 72 h

ited few char residues in the central position, while IFRC-4 showed a dense residual char in the central position after the fire resistance test. The results indicated that MFBZ and IFR jointly promoted the formation of a dense and intumescent char layer under external flame.

The char morphology was further studied by SEM, with the corresponding images shown in Figs. 5e–5h. As shown in Fig. 5e, there were some holes on the surface of residual char of IFRC-1, which was not conducive to hindering the heat transfer and smoke diffusion. Compared with IFRC-1, the char layer of IFRC-2, IFRC-3, and IFRC-4 exhibited more compact structure, and there was almost no hole on the surface. Obviously, the enhanced fire resistance and smoke suppression were mainly due to the formation of a dense and intumescent char layer with thermal shielding and smoke suppression effects.

Water resistance of coatings

In practical application, the coatings often suffered from the erosion of water and moisture. In addition, the intumescent fire-retardant coatings easily became ineffective when soaked in water for a long time. Thus, it was necessary to investigate the water resistance of intumescent fire-retardant coatings.

The water contact angles of IFRC-3, IFRC-5, IFRC-6, and IFRC-7 are shown in Fig. 6. As shown in Fig. 6, the water contact angles for IFRC-5, IFRC-6, IFRC-7, and IFRC-3 were 31.5°, 57.9°, 72.6°, and 90.1°, respectively. Clearly, the water contact angle of IFRC-3 was much larger than that of IFRC-5, which indicated that the microencapsulation contributed to suppressing the hydrophilicity of APP and BZ, and thus improving the water resistance of intumescent fire-retardant coating.

To further evaluate the water resistance of coatings, the static immersion test was performed and the status of coatings under different immersion times is shown in Fig. 7. It was obvious that IFRC-5 and IFRC-7 blistered after being soaked for only 2 h. Meanwhile, IFRC-5 and IFRC-7 were destroyed and IFRC-6 exhibited some bubbles on the surface after being soaked for 72 h. However, IFRC-3 had not been destroyed and maintained a good surface structure throughout the whole test. Obviously, the hydrophobic MF resin protected APP and BZ from being attacked by water and moisture, and thus preventing the damage of coating. The results further confirmed that the microencapsulation of APP and BZ contributed to improving the water resistance of intumescent fire-retardant coating.

The fire resistance of IFRC-5, IFRC-6, IFRC-7, and IFRC-3 before and after static immersion test was separately investigated, with the results presented in Fig. 8. As shown in Fig. 8a, IFRC-5, IFRC-6, IFRC-7, and IFRC-3 exhibited similar fire resistance before

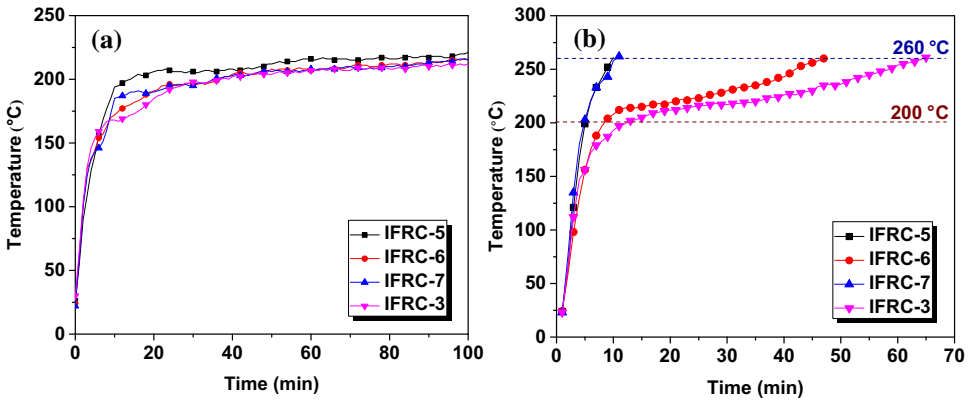

Fig. 8: The curves of backside temperature as a function of time (a) before the static immersion test and (b) after the static immersion test

static immersion test, which indicated that the microencapsulation did not impair the fire resistance. However, there were significant changes in the fire resistance after the static immersion test. Clearly, the backside temperatures of IFRC-5 and IFRC-7 increased rapidly and took only 4 min to reach above 200°C. For IFRC-6, it exhibited a certain heat insulation effect, whose backside temperature reached up to 200°C at 8 min and increased to 260°C at 46 min. After static immersion test, IFRC-3 exhibited the best fire resistance among all coatings. The backside temperature of IFRC-3 was lower than those of other three coatings throughout the test, which took 12 min and 63 min to increase to 200 and 260°C, respectively. The results further confirmed that the microencapsulation effectively reduced the loss of APP and BZ in the intumescent fire-retardant coating during static immersion test, and thus maintaining its fire resistance.

Conclusions

In this work, we successfully fabricated an intumescent coating with improved fire resistance and water tolerance via the introduction of MFAPP and MFBZ. The as-prepared coating exhibited great fire resistance and smoke suppression. Meanwhile, the addition of MFBZ imparted exceptional water resistance to the intumescent fire-retardant coating. In detail, the water contact angle of the obtained coating increased to 90.1°, and it maintained good structure and fire resistance after being soaked by water. The enhanced performance portfolio was mainly due to the synergistic flame-retardant and smoke suppression effects of MFAPP, PER, MEL, and MFBZ and the hydrophobicity of MF. This work provides a practical strategy for creating an intumescent fire-retardant coating that combines great fire resistance, smoke suppression, and water tolerance.

Acknowledgments Siqi Huo and Cheng Wang equally contribute to this work and are listed as co-first authors. This work is supported by the Foundation for Outstanding Youth Innovative Research Groups of Higher Education Institution in Hubei Province (T201706), the Foundation for Innovative Research Groups of Hubei Natural Science Foundation of China (2017CFA009), the National Natural Science Foundation of China (NSFC51973169, NSFC51903193), the China Postdoctoral Science Foundation (2018M642924), and the Hubei Province Postdoctoral Science and Technology Activity Project (G73).

References

1. Jeyasubramanian, K, Muthusankar, E, Hikku, GS, Selvakumar, N, ''Improved Thermal and Fire Retardant Behavior of Polyvinyl Alcohol Matrix Using Nanocomposites.'' *Int. J. Nanosci*., **18** 1850025 (2019)
2. Gao, Y, Wang, Q, Lin, W, ''Ammonium Polyphosphate Intercalated Layered Double Hydroxide and Zinc Borate as Highly Efficient Flame Retardant Nanofillers for Polypropylene.'' *Polymers (Basel)*, **10** 1114 (2018)
3. Shen, M-Y, Chen, W-J, Kuan, C-F, Kuan, H-C, Yang, J-M, Chiang, C-L, ''Preparation, Characterization of Microencapsulated Ammonium Polyphosphate and Its Flame Retardancy in Polyurethane Composites.'' *Mater. Chem. Phys.*, **173** 205–212 (2016)
4. Sarabandi, K, Jafari, SM, Mohammadi, M, Akbarbaglu, Z, Pezeshki, A, Khakbaz Heshmati M, ''Production of Reconstitutable Nanoliposomes Loaded with Flaxseed Protein Hydrolysates: Stability and Characterization.'' *Food Hydrocoll.*, **96** 442–450 (2019)
5. Yang, S, Wang, J, Huo, S, Cheng, L, Wang, M, ''Preparation and Flame Retardancy of an Intumescent Flame-Retardant Epoxy Resin System Constructed by Multiple Flame-Retardant Compositions Containing Phosphorus and Nitrogen Heterocycle.'' *Polymer Degrad. Stab.*, **119** 251–259 (2015)
6. Muhoza, B, Xia, S, Zhang, X, ''Gelatin and High Methyl Pectin Coacervates Crosslinked with Tannic Acid: The Characterization, Rheological Properties, and Application for Peppermint Oil Microencapsulation.'' *Food Hydrocoll.*, **97** 105174 (2019)
7. Liu, Z, Dai, M, Hu, Q, Liu, S, Gao, X, Ren, F, Zhang, Q, ''Effect of Microencapsulated Ammonium Polyphosphate on the Durability and Fire Resistance of Waterborne Intumescent Fire-Retardant Coatings.'' *J. Coat. Technol. Res*., **16** 135–145 (2018)
8. You, Y-l, Liu, C-m, Li, D-x, Liu, S-j, He, G-w, ''Tribological and Flame Retardant Modification of Polyamide-6 Composite.'' *J. Central South Univ.*, **26** 88–97 (2019)
9. Gillani, QF, Ahmad, F, Abdul Mutalib, MI, Megat-Yusoff, PSM, Ullah, S, Messet, PJ, Zia-ul-Mustafa, M, ''Thermal Degradation and Pyrolysis Analysis of Zinc Borate Reinforced Intumescent Fire Retardant Coatings.'' *Prog. Org. Coat.*, **123** 82–98 (2018)
10. Jiang, X, Li, C, Chi, Y, Yan, J, ''TG-FTIR Study on Urea-Formaldehyde Resin Residue During Pyrolysis and Combustion.'' *J. Hazard. Mater*., **173** 205–210 (2010)
11. Wei, H, Li, L, Ma, YL, Liu, RX, Meng, SY, Niu, LT, Zhang, Z, Yang, ZW, ''A Facile Method for Preparation of PGS@ZB-N and Gas-Sol Alternating Synergistic Effect for Fire Resistance of EVA.'' *Fire Mater*. **43** 868–879 (2019)
12. Savas, LA, Dogan, M, ''Flame Retardant Effect of Zinc Borate in Polyamide 6 Containing Aluminum Hypophosphite.'' *Polymer Degrad. Stab*., **165** 101–109 (2019)
13. Kumar, V, Balasubramanian, K, ''Progress Update on Failure Mechanisms of Advanced Thermal Barrier Coatings: A Review.'' *Prog. Org. Coat*., **90** 54–82 (2016)
14. Yan, L, Xu, Z, Wang, X, ''Synergistic Flame-Retardant and Smoke Suppression Effects of Zinc Borate in Transparent Intumescent Fire-Retardant Coatings Applied on Wood Substrates.'' *J. Therm. Anal. Calorim*., **136** 1563–1574 (2018)
15. Li, M, Liu, N, Li, Q, ''A Novel Core-Shell Epoxy High Performance Composite: Self-Lubricating, Heat-Resistant and Self-Repairing.'' *Prog. Org. Coat*., **129** 217–228 (2019)
16. Contri, G, Barra, GMO, Ramoa, SDAS, Merlini, C, Ecco, LG, Souza, FS, Spinelli, A, ''Epoxy Coating Based on Montmorillonite-Polypyrrole: Electrical Properties and Prospective Application on Corrosion Protection of Steel.'' *Prog. Org. Coat.*, **114** 201–207 (2018)
17. Huo, S, Liu, Z, Wang, J, ''Thermal Properties and Flame Retardancy of an Intumescent Flame-Retarded Epoxy Sys-

tem Containing Phosphaphenanthrene, Triazine-Trione and Piperidine.'' *J. Therm. Anal. Calorim.,* **139** 1099–1110 (2020)
18. Huo, S, Liu, Z, Li, C, Wang, X, Cai, H, Wang, J, ''Synthesis of a Phosphaphenanthrene/Benzimidazole-Based Curing Agent and Its Application in Flame-Retardant Epoxy Resin.'' *Polymer Degrad. Stab*., **163** 100–109 (2019)
19. Liu, S, Wang, C, Hu, Q, Huo, S, Zhang, Q, Liu, Z, ''Intumescent Fire Retardant Coating with Recycled Powder from Industrial Effluent Optimized Using Response Surface Methodology.'' *Prog. Org. Coat*., **140** 105494 (2020)
20. Islam, MR, Beg, MDH, Jamari, SS, ''Dispersion of Montmorillonite Nanoclays and Their Effects on the Thermomechanical, Structural and Drying Properties of Palm Oil Based Coating.'' *Prog. Org. Coat*., **91** 17–24 (2016)
21. Huo, S, Wang, J, Yang, S, Zhang, B, Chen, X, Wu, Q, Yang, L, ''Synthesis of a Novel Reactive Flame Retardant Containing Phosphaphenanthrene and Piperidine Groups and Its Application in Epoxy Resin.'' *Polymer Degrad. Stab.*, **146** 250–259 (2017)
22. Yang, S, Zhang, Q, Hu, Y, ''Synthesis of a Novel Flame Retardant Containing Phosphorus, Nitrogen and Boron and Its Application in Flame-Retardant Epoxy Resin.'' *Polymer Degrad. Stab*., **133** 358–366 (2016)
23. Yang, S, Wang, J, Huo, S, Wang, M, Cheng, L, ''Synthesis of a Phosphorus/Nitrogen-Containing Additive with Multifunctional Groups and Its Flame-Retardant Effect in Epoxy Resin.'' *Ind. Eng. Chem. Res*., **54** 7777–7786 (2015)
24. Yang, S, Wang, J, Huo, S, Wang, M, Wang, J, Zhang, B, ''Synergistic Flame-Retardant Effect of Expandable Graphite and Phosphorus-Containing Compounds for Epoxy Resin: Strong Bonding of Different Carbon Residues.'' *Polymer Degrad. Stab*., **128** 89–98 (2016)
25. Lu, X, Jiang, H, ''Recent Progress of Seismic Research on Tall Buildings in China Mainland.'' *Earthq. Eng. Eng. Vib.*, **13** 47–61 (2014)
26. Li, XB, ''Technical Progress and Product Development of TISCO Stainless Steel.'' 19–26 (2011)
27. Huo, S, Wang, J, Yang, S, Wang, J, Zhang, B, Zhang, B, Chen, X, Tang, Y, ''Synthesis of a Novel Phosphorus-Nitrogen Type Flame Retardant Composed of Maleimide, Triazine-Trione, and Phosphaphenanthrene and Its Flame Retardant Effect on Epoxy Resin.'' *Polymer Degrad. Stab*., **131** 106–113 (2016)
28. Chen, X, Jiang, Y, Jiao, C, ''Smoke Suppression Properties of Ferrite Yellow on Flame Retardant Thermoplastic Polyurethane Based on Ammonium Polyphosphate.'' *J. Hazard Mater.*, **266** 114–121 (2014)
29. Huo, S, Wang, J, Yang, S, Zhang, B, Tang, Y, ''A Phosphorus-Containing Phenolic Derivative and Its Application in Benzoxazine Resins: Curing Behavior, Thermal, and Flammability Properties.'' *J. Appl. Polym. Sci*., **133** (2016)
30. Camargo, Á, Ibañez, CM, ''Initial Study of Micronized Zinc Borate as Flame Retardant in Eucalyptus Grandis from Uruguay.'' *MRS Adv.*, **3** 3551–3556 (2018)
31. Song, J, Huang, Z, Qin, Y, Li, X, ''Thermal Decomposition and Ceramifying Process of Ceramifiable Silicone Rubber Composite with Hydrated Zinc Borate.'' Materials, **12** 1591 (2019)
32. Gao, Y, Liu, S, Wang, Q, Wang, G, ''Preparation of Melamine-Formaldehyde Resin Grafted by (3-Aminopropyl) Triethoxysilane for High-Performance Hydrophobic Materials.'' *J. Appl. Polym. Sci*., **137** 48664 (2020)
33. Savas, LA, Dogan, M, ''Flame Retardant Effect of Zinc Borate in Polyamide 6 Containing Aluminum Hypophosphite.'' *Polymer Degrad. Stab.*, **165** 101–109 (2019)
34. Gao, C, Moya, S, Lichtenfeld, H, Casoli, A, Fiedler, H, Donath, E, Möhwald, H, ''The Decomposition Process of Melamine Formaldehyde Cores: The Key Step in the Fabrication of Ultrathin Polyelectrolyte Multilayer Capsules.'' *Macromol. Mater. Eng*., **286** 355–361 (2001)
35. Huang, G, Huo, S, Xu, X, Chen, W, Jin, Y, Li, R, Song, P, Wang, H, ''Realizing Simultaneous Improvements in Mechanical Strength, Flame Retardancy and Smoke Suppression of ABS Nanocomposites from Multifunctional Graphene.'' *Compos. B Eng*., **177** 107377 (2019)
36. Huo, S, Yang, S, Wang, J, Cheng, J, Zhang, Q, Hu, Y, Ding, G, Zhang, Q, Song, P, ''A Liquid Phosphorus-Containing Imidazole Derivative as Flame-Retardant Curing Agent for Epoxy Resin with Enhanced Thermal Latency, Mechanical, and Flame-Retardant Performances.'' *J. Hazardous Mater*., **386** 121984 (2020)
37. Fang, F, Huo, S, Shen, H, Ran, S, Wang, H, Song, P, Fang, Z, ''A Bio-based Ionic Complex with Different Oxidation States of Phosphorus for Reducing Flammability and Smoke Release of Epoxy Resins.'' *Compos. Commun*. **17** 104–108 (2020)
38. L Yan, Z Xu, X Wang, ''Synergistic Flame-Retardant and Smoke Suppression Effects of Zinc Borate in Transparent Intumescent Fire-Retardant Coatings Applied on Wood Substrates.'' *J. Thermal Anal. Calorim*., **136** 1563–1574 (2018)
39. Kang, FR, Wang, CP, Deng, J, Yang, K, Ma, L, Pang, QT, ''Flame Retardancy and Smoke Suppression of Silicone Foams with Microcapsulated Aluminum Hypophosphite and Zinc Borate'' *Polym. Adv. Technol.*, **31** 654–664 (2020)